

SIR,

Comments on "Calculating basal thermal zones beneath the Antarctic ice sheet" by Wilch and Hughes

Wilch and Hughes (2000; hereafter WH) present a calculation of the subglacial thermal zones in parts of East and West Antarctica using Drewry's (1983) maps of ice surface and basal topography. Their calculations suggest that the ice-sheet base is "thawed" beneath Dome C, in central East Antarctica, across the Vincennes Subglacial Basin, but in their figure 12 a large region of frozen-based ice has been drawn for this area. The figure caption has been miswritten, and the correct denotation of melting and freezing zones should be "horizontal lines are complete subglacial melt zones, and vertical lines are complete freeze zones".

A comparison between WH's calculations and maps, and the locations of subglacial lakes in this region of Antarctica is quite interesting (Fig. 1). Regions where WH calculated that the ice-sheet base was completely thawed are closely related to the position of many known subglacial lakes. Subglacial lakes are pockets of water stored within topographic hollows beneath the ice sheet. They can be readily identified on airborne radio-echo sounding (RES) records since they have a characteristic flat, bright, near-horizontal radar reflection, compared with the weaker, undulating signal reflected from ice-bedrock interfaces. An inventory of Antarctic subglacial lakes (Siegert and others, 1996) shows the locations of 77 known subglacial lakes in the region of the Scott Polar Research Institute RES survey (i.e. the same region as that investigated by WH). Beneath Dome C the 40 or so known subglacial lakes are mostly <12 km long and occupy <10% of the total subglacial area in this region (Siegert and Ridley, 1998). The lakes are often located across the flanks of deep, extensive troughs like the Vincennes Subglacial Basin, the Aurora Subglacial Basin and the Adventure Subglacial Trench. Since relatively thicker ice will have a lower sub-

glacial pressure-melting point, lakes located at the elevated flanks of deep troughs can be interpreted as evidence for subglacial melting across a much wider region (i.e. across the deep troughs) than just their surface areas. The wider distribution of subglacial lakes is even more compatible with the results of WH, since even a predominantly frozen zone will contain a thawed fraction to accommodate a pool of subglacial water. No subglacial lakes are positioned within regions where the WH model shows a completely frozen bed.

The Drewry (1983) map of surface elevation used by WH has been much improved in the last 17 years. For example, European Remote-sensing Satellite 1 (ERS-1) altimetry of the region provides much more accurate ice-surface slopes (Bamber and Bindshadler, 1997), and the new BEDMAP depiction of the ice-sheet basal elevation (Lythe and others, 2000) is also much improved. Many relatively large (>30 km wide) low-sloping ice-surface features found in the ERS-1 data overlie either known subglacial lakes around Dome C (Siegert and Ridley, 1998) or regions interpreted as water-saturated sediment pockets (Siegert, 2000). Further, a model of ice-sheet flux, using these recent datasets as input, shows that several subglacial lakes are located close to the onset of enhanced ice flow (Siegert and Bamber, 2000) and suggests that a number of ice-flow units in Antarctica may be subglacially thawed. It would be interesting to see if the WH calculations, driven with these newer input data, would match (1) the known distribution of subglacial lakes better than the match shown in Figure 1, and (2) the distribution of warm-based ice-flow units.

Bristol Glaciology Centre,
School of Geographical Sciences,
University of Bristol,
Bristol BS8 1SS, England

MARTIN J. SIEGERT

5 March 2001

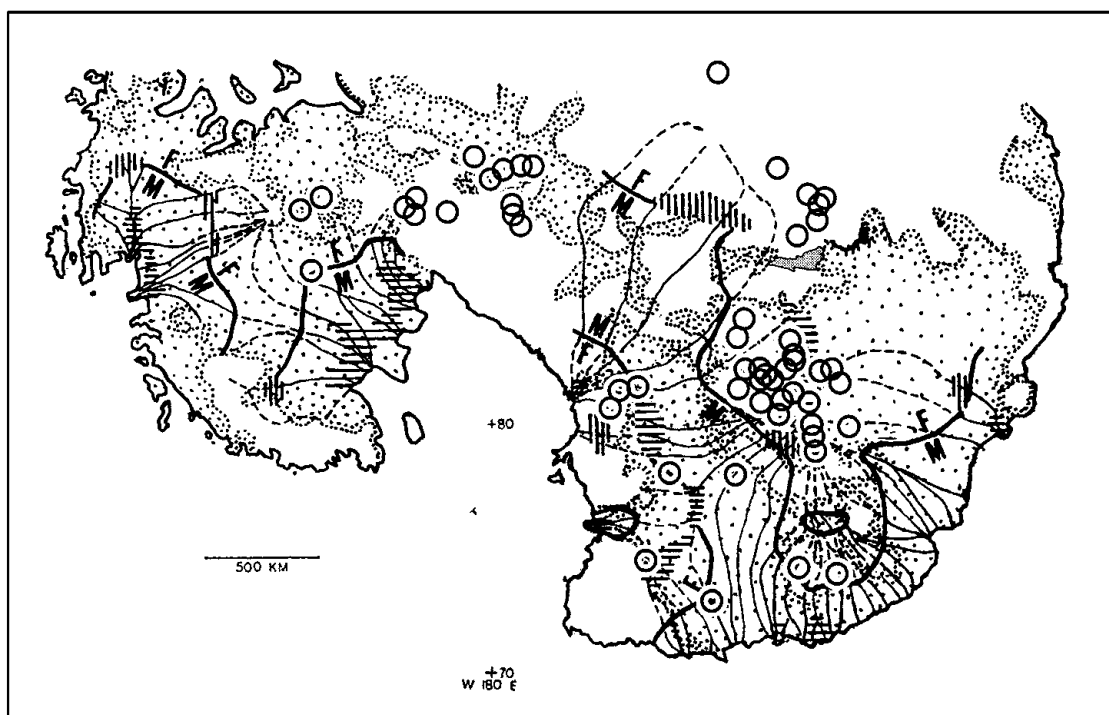


Fig. 1. The distribution of Antarctic subglacial lakes, denoted as circles (the centre of each marks the lake location) (Siegert and others, 1996), superimposed over figure 12 of WH, in which the location of calculated subglacial freezing and melting zones is denoted. Lake Vostok is outlined and shaded. Horizontal lines indicate regions where $f = 1$ (complete thawing), whilst vertical lines represent areas where $f = 0$ (no thawing).

REFERENCES

Bamber, J. L. and R. A. Bindschadler. 1997. An improved elevation dataset for climate and ice-sheet modelling: validation with satellite imagery. *Ann. Glaciol.*, **25**, 439–444.

Drewry, D. J., ed. 1983. *Antarctica: glaciological and geophysical folio*. Cambridge, University of Cambridge. Scott Polar Research Institute.

Lythe, M. B., D. G. Vaughan and BEDMAP consortium. 2000. *BEDMAP—bed topography of the Antarctic*. Scale 1:10 000 000. British Antarctic Survey. (BAS (Misc) 9).

Siegert, M. J. 2000. Radar evidence of water-saturated sediments beneath the central Antarctic ice sheet. In Maltman, A. J., B. Hubbard and M. J. Hambrey, eds. *Deformation of glacial materials*. London, Geological Society, 217–229. (Special Publication 176.)

Siegert, M. J. and J. L. Bamber. 2000. Correspondence. Subglacial water at the heads of Antarctic ice-stream tributaries. *J. Glaciol.*, **46**(155), 702–703.

Siegert, M. J. and J. K. Ridley. 1998. Determining basal ice-sheet conditions in the Dome C region of East Antarctica using satellite radar altimetry and airborne radio-echo sounding. *J. Glaciol.*, **44**(146), 1–8.

Siegert, M. J., J. A. Dowdeswell, M. R. Gorman and N. F. McIntyre. 1996. An inventory of Antarctic sub-glacial lakes. *Antarct. Sci.*, **8**(3), 281–286.

Wilch, E. and T. J. Hughes. 2000. Calculating basal thermal zones beneath the Antarctic ice sheet. *J. Glaciol.*, **46**(153), 297–310.

SIR,

Complexity of the climatic regime over the Lambert Glacier basin of the East Antarctic ice sheet: firn-core evidences

Deep ice-core records from Antarctica and Greenland indicate rather similar climate histories over long time-scales (Bender and others, 1994; Jouzel, 1994; Kreutz and others, 1997), but over decadal to centennial scales the records from different regions of the Antarctic ice sheet show large differences. For instance, although increasing accumulation rates have been reported for many sites (Pourchet and others, 1983; Peel and Mulvaney, 1988; Morgan and others, 1991; Mosley-Thompson and others, 1995), several sites show decreasing trends (Graf and others, 1990; Kameda and others, 1990; Bindschadler and others, 1993; Isaksson and Karlén, 1994; Ren and others, 1999). A similar situation is apparent in isotope temperature records (Isaksson and others, 1996; Ren and others, 1999). Here, we discuss firn-core records of accumulation and isotopic trends since 1940 deduced from the top

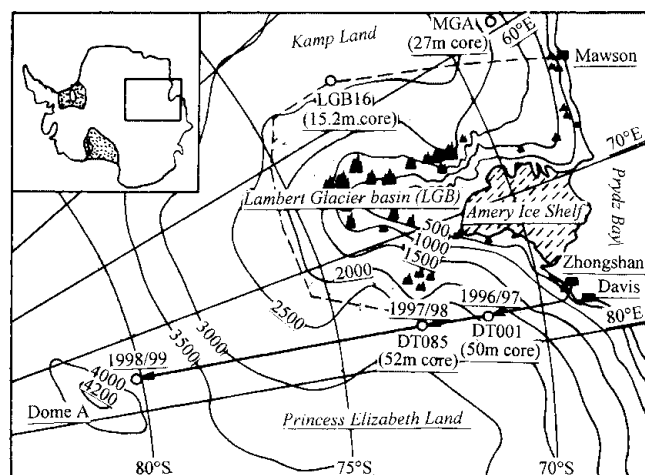


Fig. 1. Location map of the firn cores (empty circles) drilled over the LGB. The solid line is the traverse route of the Chinese National Antarctic Research Expedition (CHINARE), and the dashed line is the route of the Australian National Antarctic Research Expedition (ANARE).

sections of four cores drilled on the west and east sides of the Lambert Glacier basin (LGB; Fig. 1).

During the 1992 joint Australian–Chinese over-snow traverse on the west side of the LGB, we drilled two firn cores, MGA (68°39' S, 60°15' E; 1830 m a.s.l.) and LGB16 (72°49' S, 57°20' E; 2689 m a.s.l.), 27 and 15 m long, respectively. These cores were dated stratigraphically using isotopic profiles, electrical conductivity measurements, stratigraphy and known accumulation rates. A series of firn cores were drilled adjacent to each of the two sites to check the precision of the dating (Ren and others, 1999). Between 1996 and 1998, a second pair of firn cores were extracted, DT001 (71°51' S, 77°55' E; 2325 m a.s.l.) and DT085 (73°22' S, 77°01' E; 2577 m a.s.l.), 50 and 52 m long, respectively. $\delta^{18}\text{O}$ and chemical series (Cl^- , Na^+ and NO_3^-) were used to cross-date these with a precision believed to be ± 2 years for the upper 20 m (Qin and others, 2000). Only top sections of these latter two cores were used in order to match roughly

Table 1. Comparison of decadal accumulation and $\delta^{18}\text{O}$ values in the firn cores at MGA, LGB16, DT001 and DT085; the rates of change in accumulation and $\delta^{18}\text{O}$ since 1940 are also listed

Firn core and time period	Mean accumulation rate		Mean $\delta^{18}\text{O}$	
	kg m ⁻² a ⁻¹	Deviation from average %	Deviation from average %	Deviation from average %
		%	‰, V-SMOW*	‰
MGA				
1940–49	345.8	+24.5	-35.73	+0.13
1950–59	296.1	+6.6	-35.93	-0.07
1960–69	275.6	-0.7	-36.87	-1.01
1970–79	249.8	-10.0	-35.02	+0.84
1980–89	246.5	-11.2	-35.76	+0.10
1990–92	238.7		-35.16	
1940–92	277.7	-2.4 kg m ⁻² a ⁻¹ (rate of change)	-35.86	+0.015‰ a ⁻¹ (rate of change)
LGB16				
1940–49	148.7	+20.9	-43.80	+0.53
1950–59	112.6	-8.5	-44.51	-0.18
1960–69	136.4	+10.9	-43.94	+0.39
1970–79	106.0	-13.7	-45.55	-1.22
1980–89	106.1	-13.7	-44.83	-0.50
1990–92	140.3		-42.85	
1940–92	123.0	-0.7 kg m ⁻² a ⁻¹ (rate of change)	-44.33	-0.011‰ a ⁻¹ (rate of change)
DT001				
1940–49	135.2	+2.8	-38.89	-0.76
1950–59	131.0	-0.3	-37.73	+0.43
1960–69	92.5	-70.0	-38.67	-0.54
1970–79	142.3	+8.0	-38.44	-0.31
1980–89	154.6	+17.6	-37.35	+0.78
1990–96	133.7	+1.7	-37.57	+0.56
1940–96	131.4	+0.3 kg m ⁻² a ⁻¹ (rate of change)	-38.13	+0.025‰ a ⁻¹ (rate of change)
DT085				
1940–49	151.6	-1.1	-41.15	-0.13
1950–59	155.8	+1.6	-42.09	-1.07
1960–69	93.8	-38.8	-39.98	+1.04
1970–79	149.0	-2.8	-41.43	-0.41
1980–89	178.8	+16.6	-40.60	+0.42
1990–97	160.0	+4.4	-40.62	+0.40
1940–97	153.3	+1.2 kg m ⁻² a ⁻¹ (rate of change)	-41.02	+0.017‰ a ⁻¹ (rate of change)

* Vienna Standard Mean Ocean Water.